Arginine-Terminated Generation 4 PAMAM Dendrimer as an Effective Nanovector for Functional siRNA Delivery in Vitro and in Vivo

ARTICLE *in* BIOCONJUGATE CHEMISTRY · FEBRUARY 2014

Impact Factor: 4.51 · DOI: 10.1021/bc4005156 · Source: PubMed

6 AUTHORS, INCLUDING:

Cheng Liu
Kunming University of Science and Technolo…
138 PUBLICATIONS **2,970** CITATIONS
SEE PROFILE

Xiaoxuan Liu
Aix-Marseille Université
21 PUBLICATIONS **463** CITATIONS
SEE PROFILE

Ling Peng
CINaM - Centre Interdisciplinaire de Nanosci…
115 PUBLICATIONS **2,242** CITATIONS
SEE PROFILE

Bioconjugate Chemistry

Article

pubs.acs.org/bc

Arginine-Terminated Generation 4 PAMAM Dendrimer as an Effective Nanovector for Functional siRNA Delivery in Vitro and in Vivo

Cheng Liu,[†,‡] Xiaoxuan Liu,[*,‡] Palma Rocchi,[∥,§,⊥,#] Fanqi Qu,[†] Juan L. Iovanna,[∥,§,⊥,#] and Ling Peng[*,‡]

[†]State Key Laboratory of Virology, College of Chemistry and Molecular Sciences, Wuhan University, Wuhan 430072, P. R. China

[‡]Aix-Marseille Université, CNRS UMR 7325, Centre Interdisciplinaire de Nanoscience de Marseille, 13288 Marseille, France

[§]Institut Paoli-Calmettes, 13009 Marseille, France

[∥]Centre de Recherche en Cancérologie de Marseille, Inserm, UMR1068, 13009 Marseille, France

[⊥]Aix-Marseille Université, 13284 Marseille, France

[#]CNRS, UMR7258, 13009 Marseille, France

Supporting Information

ABSTRACT: Successful therapeutic implementation of RNA interference critically depends on systems able to safely and efficiently deliver small interfering RNA (siRNA). Dendrimers are emerging as appealing nanovectors for siRNA delivery by virtue of their unique well-defined dendritic nanostructure within which is confined an intriguing cooperativity and multivalency. We have previously demonstrated that structurally flexible triethanolamine (TEA) core poly(amidoamine) (PAMAM) dendrimers of high generations are effective nanovectors for siRNA delivery in vitro and in vivo. In the present study, we have developed arginine-terminated dendrimers with the aim of combining and harnessing the unique siRNA delivery properties of the TEA-core PAMAM dendrimer and the cell-penetrating advantages of the arginine-rich motif. A generation 4 dendrimer of this family (**G_4Arg**) formed stable dendriplexes with siRNA, leading to improved cell uptake of siRNA by comparison with its nonarginine bearing dendrimer counterpart. Moreover, **G_4Arg** was demonstrated to be an excellent nanocarrier for siRNA delivery, yielding potent gene silencing and anticancer effects in prostate cancer models both in vitro and in vivo with no discernible toxicity. Consequently, importing an arginine residue on the surface of a dendrimer is an appealing option to improve delivery efficiency, and at the same time, the dendrimer **G_4Arg** constitutes a highly promising nanovector for efficacious siRNA delivery and holds great potential for further therapeutic applications.

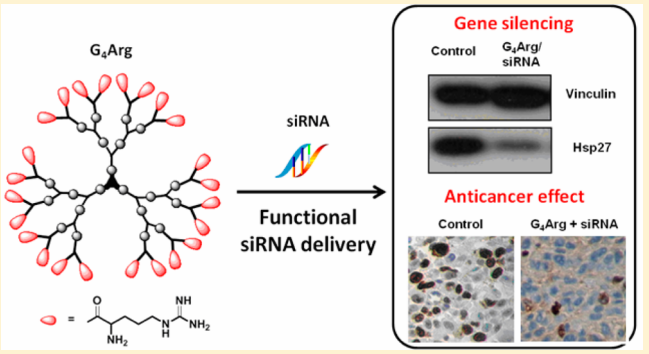

INTRODUCTION

Since the discovery of RNA interference (RNAi),[1] small interfering RNAs (siRNAs) have emerged as a promising therapeutic modality to silence disease-associated genes.[2−4] The main obstacles facing the development of such therapeutics is the susceptibility of siRNA molecules to degradation by various enzymes and the difficulty with which they can cross the cell membrane due to their negatively charged and hydrophilic phosphate backbones as well as their relatively large molecular weight (∼14 kDa). Consequently, the successful therapeutic implementation of RNAi depends on the availability of safe and efficient delivery systems able to prevent siRNAs from degradation and bring them to the site of interest. The recent boom in the development of nanotechnology has resulted in a flourishing of nanovectors for siRNA delivery, both natural and synthetic, including liposomes, synthetic organic polymers (e.g., polyethylenimine, dendrimers, and cyclodextrins), and inorganic materials (e.g., carbon nanotubes, quantum dots, and gold nanoparticles).[5−7] Among these, dendrimers, a family of synthetic macromolecules,[8] represent a particularly promising siRNA delivery platform[9−11] by virtue of their precisely controlled radial symmetrical structure, intriguing multivalency, and high cargo payload confined within a nanoscale volume. We have hence developed structurally flexible poly(amidoamine) (PAMAM) dendrimers featuring an extended triethanolamine (TEA) core for siRNA delivery.[11,12] These dendrimers bear positively charged amine functionalities at the surface, which are responsible for ionic condensation with the negatively charged siRNA molecules. At the same time, these dendrimers also harbor tertiary amines

Received: November 3, 2013
Revised: February 3, 2014

   dx.doi.org/10.1021/bc4005156 | *Bioconjugate Chem.* XXXX, XXX, XXX−XXX

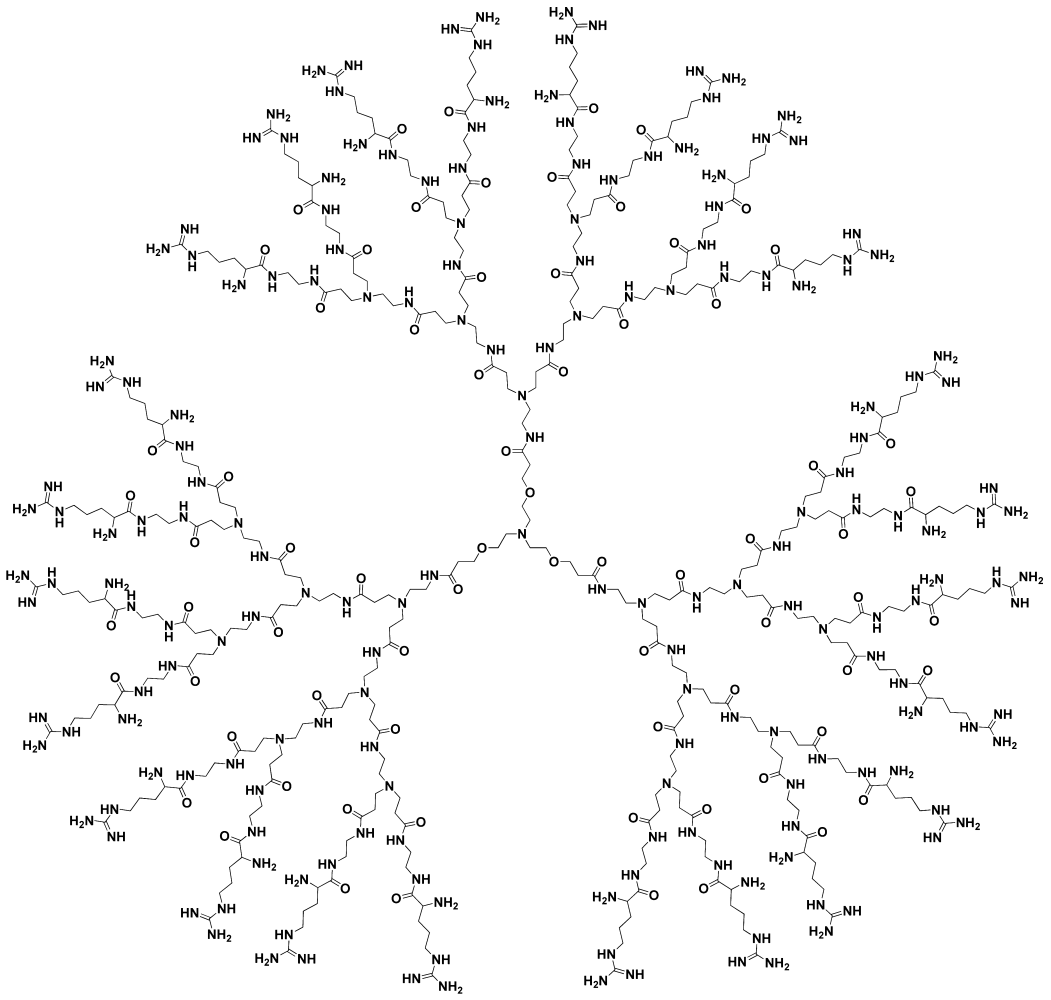

Figure 1. Chemical structure of an arginine-terminated TEA-core PAMAM dendrimer of generation 3 (**G_3Arg**).

within their interior, which can preferentially promote the intracellular release of siRNA via the "proton sponge" effect. Importantly, the larger and extended TEA core conveys a more flexible structure to the dendrimers that have less densely packed branching units and are hence more accessible to water and nucleic acid molecules, thus favoring both binding and release of nucleic acid.[13] High generation dendrimers of this family are excellent nanovectors able to deliver siRNA therapeutics in different disease models both in vitro and in vivo,[14−20] and demonstrate great potential for further clinical applications. Notwithstanding, the large-scale synthesis of high generation dendrimers is technically demanding, and meeting the "good manufacturing practice" (GMP) grade required for further clinical trials is difficult. Consequently, developing lower generation dendrimers of this family via structural modification which imparts effective delivery activity while conserving flexible structure constitutes a worthwhile goal.

Recently, several arginine-rich peptides, known as cell-penetration peptides (CPPs), such as transactivator of transcription (TAT),[21] penetratin,[22] and oligoarginine,[23] have been intensively described for their outstanding transmembrane translocation ability.[24] The arginine residues[25−27] are double positively charged in physiological conditions due to the presence of both a guanidinium group and a primary amine functionality. They can favorably interact with the negatively charged cell membrane-associated proteoglycans, thus intensifying membrane penetration.[28,29] The conjugation of arginine-rich motifs to various drug delivery vehicles has indeed proven beneficial in enhancing cellular uptake.[30] Such a strategy can be exploited to design arginine-bearing vectors for the delivery of siRNA therapeutics with the aim of increasing cellular uptake and consequently enhanced siRNA delivery and improved gene silencing.

With this in mind, we wished to harness the cell-penetrating advantages of arginine-rich motifs to empower low generation dendrimers with effective siRNA delivery properties. Accordingly, we wanted to conjugate arginine components onto the surface of our TEA-core PAMAM dendrimer. On the basis of the multivalent property of dendrimers, we reasoned that, instead of long arginine-rich peptide segments, we can simply append the dendrimer terminals with single arginine units (Figure 1), and as such the resulting dendrimers could be considered as arginine-rich nanovectors able to conserve the cell penetration advantage of arginine-rich motifs while maintaining the structural flexibility of the TEA-core PAMAM dendrimers. We report below our study on a set of such low generation dendrimers composed of the backbone of TEA-core PAMAM dendrimers with peripheries decorated by arginine residues, with regard to their ability as nanovectors for siRNA delivery. Indeed, a small arginine-terminated dendrimer of as low as generation 4 (**G_4Arg**) was able to effectively deliver siRNA by way of the improved cell-penetration ability imparted

dx.doi.org/10.1021/bc4005156 | *Bioconjugate Chem.* XXXX, XXX, XXX−XXX

by the arginine components, resulting in potent gene silencing and anticancer activity in prostate cancer models in vitro and in vivo. Effectively, the decoration of the dendrimer terminals with arginine residues appears to boost low generation dendrimers with effective siRNA delivery ability. To our knowledge, this is the first successful report on an arginine-decorated dendrimer with such a significant invigoration for siRNA delivery.

EXPERIMENTAL PROCEDURES

Materials. Amine-terminated TEA-core PAMAM dendrimers were synthesized according to the previously reported method.[12] Fmoc-Arg(pbf)-OH, 1-hydroxybenzotriazole (HOBt), *O*-(benzotriazol-1-yl)-*N*,*N*,*N*′,*N*′-tetramethyluronium hexafluorophosphate (HBTU) and *N*,*N*-diisopropylethylamine (DIPEA) were purchased from Acros Organics (Illkirch, France), Sigma Aldrich (Saint-Quentin Fallavier, France), or Alfa Aesar (Ward Hill, MA, USA). The sequence of heat shock protein 27 (Hsp27) siRNA used corresponds to the human Hsp27 site (5′-GCUGCAAAAUCCGAUGAGACdTdT-3′) (Thermo Fisher Scientific, Illkrich, France). A scrambled siRNA duplex (Thermo Fisher Scientific) (5′-AUCAA-ACUGUUGUCAGCGCUGdTdT-3′) and Dy647-labeled Hsp27 were purchased from Thermo Fisher Scientific. The TPT1 siRNA targeting translationally controlled tumor protein (TCTP) (Cat. No. SI02664179) was purchased from Qiagen (Courtaboeuf, France). Oligofectamine was purchased from Invitrogen (Paisley, United Kingdom). All other reagents and solvents of analytical grade were used without any further purification from commercial sources.

Synthesis of TEA-Core Arginine-Terminated PAMAM Dendrimers. Arginine-terminated TEA-core PAMAM dendrimers were synthesized by conjugating Fmoc-Arg(pbf)-OH to the peripheries of amine-terminated PAMAM dendrimers with the HOBt/HBTU coupling method as shown in Figure 1. Briefly, to a solution of 4.0 equiv of HOBt, 4.0 equiv of HBTU, 4.0 equiv of Fmoc-Arg(pbf)-OH, and 8.0 equiv of DIPEA (equivalent to one primary amine terminal of the amine-terminated dendrimer) in 5.0 mL of anhydrous DMF was added a solution of 50 mg of amine-terminated TEA-core PAMAM dendrimer in 5.0 mL of DMF. The reaction solution was stirred at 25 °C for 2 days. The resulting product was then precipitated with methanol/diethyl ether (1.0 mL/20 mL) at 4 °C for 12 h (three times). The residual precipitate was dissolved in 3.0 mL of DMF and mixed with a solution of 3.0 mL of 30% piperidine in DMF (v/v), then stirred at 25 °C for 2 h to deprotect the Fmoc groups. The resulting product was then precipitated with methanol/diethyl ether (1.0 mL/20 mL) at 4 °C for 12 h (three times). A solution of 7.6 mL of trifluoroacetic acid (TFA), 2.0 mL of triisopropylsilane (TIS), and 2.0 mL of water (95:2.5:2.5, v/v/v) was used to remove the pbf groups at 25 °C for 1 h. The resulting crude product was purified by the dialysis in water (800−1000 mL) (dialysis protocol: at the beginning, the water was changed every 1 h three times, then every 2−3 h three times). The dialyzed product was lyophilized to yield the corresponding arginine-terminated dendrimer. The number of arginine units decorated on the dendrimer surface could be assessed based on the characteristic ^{1}H NMR signals (4.0 ppm) of the arginine residues and their corresponding integrations compared to the specific NMR peaks (2.6 ppm) belonging to the PAMAM structure. The obtained results indicate that the peripheral primary amines of PAMAM dendrimers were almost quantitatively conjugated with arginine residues.

Potentiometric pH Titration. The solution of dendrimer (1 μmol in 10 mL) was adjusted to pH around 2−3 with 0.5 M HCl, and pH titration was carried out with 0.1 M NaOH using a Mettler Toledo 320-S pH meter.

Agarose Gel Analysis of siRNA/Dendrimer Complexes. Dendrimers were diluted to an appropriate concentration in 50 mM Tris-HCl buffer (pH 7.4), with all solutions stored at 4 °C. The siRNA was diluted with H_2O. Both solutions were mixed at various N/P ratios and incubated at 37 °C for 30 min. The final concentration of siRNA was adjusted to 25 ng/mL (100 ng/well). siRNA/dendrimer complexes were analyzed by electrophoretic mobility-shift assays in 2% agarose gel in 0.5× TBE buffer. The siRNA bands were stained by Syber green (Life Technologies SAS, Saint Aubin, France) then detected by Fujifilm LAS-3000 Imager (FUJIFILM, Bois d'Arcy, France).

Dynamic Light Scattering (DLS) Analysis. The siRNA solution was mixed with the indicated amount of freshly prepared dendrimer solution at an N/P ratio of 10. The final concentration of the siRNA was 1 μM. After incubation at 25 °C for 30 min, size distribution and zeta potential measurements were performed using Zetasizer Nano-ZS (Malvern Ltd., Malvern, Orsay, France) with a He−Ne ion laser of 633 nm.

Cell Culture. Human prostate cancer PC-3 cells were purchased from the American Type Culture Collection (Molsheim, France), and the human CR prostatic cancer cell line C4-2 was a gift from Pr. Martin Gleave (The Vancouver Prostate Centre, Canada). Breast cancer cell line MDA-MB431 was a gift from Dr. Daniel Birnbaum and Mr. Julien Wicinski (Institut Paoli-Calmettes, Marseille, France). PC-3 cells were maintained in DMEM (Invitrogen Ltd., Paisley, United Kingdom), supplemented with 10% fetal bovine serum (FBS). C4-2 cells were maintained in RPMI 1640 (Invitrogen), supplemented with 10% FBS. MDA-MB431 cells were maintained in RPMI 1640 (Invitrogen), supplemented with 10% FBS, MEM non-essential amino acids (NEAA) (Life technologie SAS), HEPES (Life technologie SAS), and ANTI−ANTI (Life technologie SAS). Cells were maintained at 37 °C in a 5% CO_2 humidified atmosphere.

Flow Cytometry. Briefly, PC-3 cells were plated in 3.5 cm dishes and treated with Dy647-labeled Hsp27 siRNA/**G_4Arg**, using no treatment and Dy647-labeled Hsp27 siRNA/**G_4** as controls. The cells were trypsinized after treatment and washed once with cold PBS. The fluorescent intensity of cells was analyzed by using a flow cytometer (Beckman Coulter Epics Elite, Beckman Coulter, Inc., Marseille, France). The comparison of median fluorescence intensity (MFI) between Dy647 Hsp27 siRNA/**G_4Arg** and Dy647-labeled Hsp27 siRNA/**G_4** was obtained using FlowJo software. Each assay was performed in triplicate.

In Vitro Transfection Experiments. One day before transfection, 1.5×10^5 cells were seeded in 6 cm dishes in 4 mL of fresh complete medium containing 10% FBS. Before transfection, a solution of the siRNA/dendrimer and siRNA/oligofectamine complex was prepared accordingly. The desired amount of siRNA and dendrimers or oligofectamine was diluted in 200 μL of Opti-MEM transfection medium. The solutions were mixed by vortexing for 10 s and then equilibrated for 10 min at room temperature. The dendrimers or oligofectamine was added to the siRNA solution, homogenized for 10 s with a vortex, and equilibrated 30 min at room temperature. Then 1.6 mL of serum-free medium was added into the complex solution and the final volume brought

dx.doi.org/10.1021/bc4005156 | *Bioconjugate Chem.* XXXX, XXX, XXX−XXX

to 2 mL. Before addition of the transfection complexes, the complete medium with FBS was removed, and cells were washed with PBS once. Then, 2 mL of complex solution was added and incubated at 37 °C in the absence of 10% FBS. After 8 h of incubation, the transfection mixture was replaced with the complete medium containing 10% FBS and maintained under normal growth conditions for further incubation of 72 h.

Quantitative Real-Time (qRT)-PCR. The expression of the Hsp27 mRNAs was analyzed by quantitative real-time PCR amplification analysis. Total RNAs were isolated using AllPrep DNA/RNA/Protein Mini Kit (Qiagen) from PC-3 cells. Then 1 μg of RNAs was reverse-transcribed into cDNA by using a ImProm-II Reverse Transcription system (Promega, Charbonnieres, France) (0.5 μg of oligo dT primer, 1 μL of ImProm-II reverse transcriptase, 0.5 μL of RNase inhibitor, 1 μL of 10 mM dNTP mix, 4.8 μL of 25 mM $MgCl_2$, and 4 μL of 5 × RT buffer) in a final volume of 20 μL. The thermal cycling protocol employed included two steps (step 1, 70 °C for 5 min, and 4 °C for 5 min; step 2, 25 °C for 5 min, 42 °C for 1 h, 70 °C for 15 min, and 4 °C forever).

The real time PCR was conducted using a LightCycler 2.0 instrument (Roche Diagnostics, GmbH Mannheim, Germany). Reaction mixtures contained a total volume of 20 μL consisting of 5 μL of each diluted cDNA (1:10), 10 μL of SYBR Premix Ex Taq (2×) (TaKaRa Bio. Inc., Japan), 0.4 μL of primers F and primers R (10 μM) of target gene Hsp27 and internal control 18S, and 4.2 μL of H_2O. The sequences of primers are as follows: Hsp27 primer F, 5′-TCCCTGGATGTCAACC-ACTTC-3′, and primer R, 5′-TCTCCACCACGCCATCCT-3′; 18S primer F, 5′-CTACCACATCCAAGGAAGGC-3′, and primer R, 5′-TTTTCGTCACTACCTCCCCG-3 (Eurogentec S. A., Seraing, Belgium). The conditions were as follows: an initial denaturation step at 95 °C for 10 s; then 45 cycles of 95 °C for 5 s, 57 °C for 6 s, and 72 °C for 12 s. A melting curve was carried out after the amplification program by heating at temperatures from 65 to 95 °C in 1.5 min. A final cooling step at 40 °C for 1 min was performed. Each sample was analyzed in triplicate in the PCR reaction to estimate the reproducibility of data. The data was acquired by using Roche Molecular Biochemicals light cycler software, version 3.5, and statistical analysis was performed by RelQuant (Roche).

Western Blot Analysis. Samples containing equal amounts of protein (15 μg) from lysates of cultured PC-3 cells or tumors were analyzed by Western blot analysis as described previously[31] with 1:5000-diluted antihuman Hsp27 rabbit polyclonal antibody (Enze Life Sciences, Villeurbanne, France) or 1:2000-diluted antihuman vinculin mouse monoclonal antibody (Sigma Aldrich). Filters were then incubated for 1 h at room temperature with 1:5000-diluted horseradish peroxidase conjugate antirabbit or mouse monoclonal antibody (Santa Cruz Biotechnology Inc., Nanterre, France). Specific proteins were detected using an enhanced chemiluminescence Western blotting analysis system (GE Healthcare Life Sciences, Velizy-Villacoublay, France).

Measurement of Caspase-3 Cleavage. Caspase-3 cleavage was detected by Western blotting as described above using 100 μg of protein. Polyclonal antibody caspase-3 and cleaved caspase-3 (Cell Signaling Technology Inc., Beverly, MA, USA) were used to detect full-length (M_r = 32 000−35000) and the large fragment of activated caspase-3 (M_r = 17 000−20000), which results from cleavage at residue Asp175.

MTT (3-(4,5-Dimethylthiazol-2-yl)-2,5-diphenyl Tetrazolium Bromide) and Crystal Violet Assay. The growth inhibitory effects of Hsp27 siRNA plus **G_4Arg** on PC-3 cells were assessed using the MTT and crystal violet assay (Sigma Aldrich, France). Briefly, cells were seeded in each well of 12-well microtiter plates and allowed to attach overnight. Cells were then treated once with dendrimer **G_4Arg**, Hsp27 siRNA/**G_4Arg**, and scramble/**G_4Arg** in the absence of 10% FBS for 8 h. Every 24 h over a period of 7 days, for the MTT assay, the MTT solution (5 mg/mL in PBS) was added to each well and incubated for another 2−4 h. Then, the suspension liquid was removed, and cells were resuspended in DMSO. The optical density (OD) of these DMSO solutions was read at 540 nm. For the crystal violet assay, the cells were fixed with 10% glutaraldehyde solution for 10 min at room temperature, then washed gently twice with distilled water. The 0.5% crystal violet solution was added into each well and incubated 5 min at room temperature. We then washed off the excess crystal violet by adding in a large volume of water with a transfer pipet, swirling and removing until the water stayed relatively clear (3−6 times). The plate was drained upside down on paper towels, then Sorensen solution was added to solubilize the stain, and the plate was agitated on an orbital shaker for 5 min until the color was uniform with no areas of dense coloration at the bottom of wells. The OD of these solutions was read at 540 nm. The difference of OD values between treated and nontreated cells reflects the viability of cells after treatments and thus stands for metabolite toxicity. Each assay was performed in triplicate.

Lactate Dehydrogenase (LDH) Assay. PC-3 cells were seeded by 5000 cells per well in 96-well plates and cultured overnight. The cells were treated with siRNA/**G_4Arg** for 8 h in the absence of 10% fetal bovine serum. After 1, 2, 4, and 24 h, the LDH concentration was measured by using a commercial LDH kit (Cytotoxicity Detection Kit, Roche, Roche Diagnostics GmbH, Meylan, France). The LDH reaction mixture was freshly prepared according to the manufacturer's protocol (Roche Diagnostics GmbH), 100 μL of LDH reaction mixture was added to each well of a 96-well plate containing 100 μL of treated cells and controls (cell with medium or lysis buffer), and the plate was incubated for 30 min at 25 °C. Controls were performed with lysis buffer and medium, and set as 100% and 0% LDH release, respectively. The relative LDH release is defined by the ratio of LDH released over total LDH in the intact cells. All samples were run in triplicate.

Assessment of in Vivo Gene Silencing and Antiproliferation. Institutional guidelines for the proper and humane use of animals in research were followed. Approximately 10 × 10^6 PC-3 cells were inoculated subcutaneously with 0.1 mL of DMEM which was supplemented with 10% FBS in the flank region of 5-week-old male xenograft nude mice (Charles River Laboratories International, Inc. France) via a 27-gauge needle. When PC-3 tumors reached 100 mm^3, usually 3 to 4 weeks after injection, mice were randomly selected for treatment with Hsp27 siRNA/**G_4Arg**, scramble/**G_4Arg**, Hsp27 siRNA alone, **G_4Arg** alone, or PBS buffer alone. Each experimental group consisted of 5 mice. After randomization, PBS buffer, 3 mg/kg Hsp27 siRNA, **G_4Arg** at an N/P ratio = 5, Hsp27 siRNA/**G_4Arg**, or scramble/**G_4Arg** complexes were injected intratumorally twice per week for two weeks. After two weeks of treatments, mice were sacrificed, and tumors were removed from the animals and divided into two parts. One part of the tumors was frozen in dry ice and then stored at −80 °C for protein extraction. The in vivo expression of Hsp27 protein was measured by Western blot as described before. Another part of

dx.doi.org/10.1021/bc4005156 | Bioconjugate Chem. XXXX, XXX, XXX−XXX

Scheme 1. Synthesis of Arginine-Terminated Dendrimers Using Amine-Terminated TEA-Core PAMAM Dendrimers

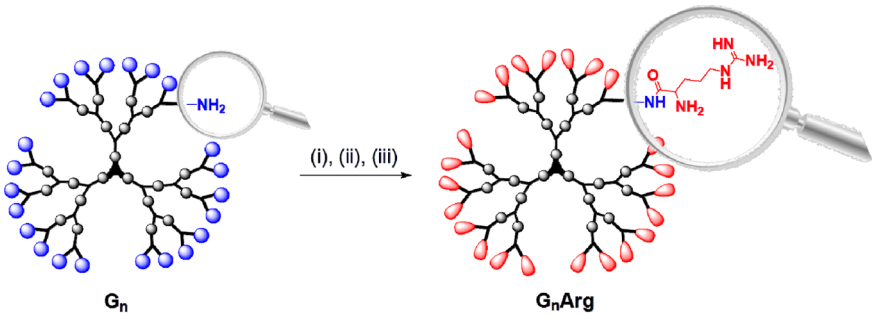

(i) Fmoc-Arg(pbf)-OH, HOBt, HBTU, DIPEA, DMF, r.t., (ii) 30% piperidine/DMF, (v/v), r.t., (iii) TFA/triisopropylsilane/H_2O = 95/2.5/2.5, (v/v/v), r.t.

the tumors was fixed in 4% paraformaldehyde at 4 °C for immunohistochemistry.

Immunohistochemistry. Three-micrometer sections were dried overnight at room temperature. Prior to antibody staining, the slides were incubated for 1.5 h at 65 °C, then incubated for 20 min at 95 °C with EnVision FLEX Target Retrieval Solution (low pH, pH 6) (K8005; Dako UK Ltd., Cambridgeshire, U.K.), then pretreated with Epitope Retrieval Solution (containing detergent) (K5207; Dako UK Ltd.) for 30 min at room temperature to unmask binding epitopes. After blocking of endogenous peroxidase activity with DAKO EnVision FLEX Peroxidase-Blocking Reagent SM801 (ready to use) (K8000, K8002, K8023; Dako UK Ltd.) for 5 min, slides were washed thoroughly in wash buffer FLEX (Dako UK Ltd.). After one wash in wash buffer FLEX, the slides were incubated with a FLEX Monoclonal Mouse Anti-Human K_i-67 Antigen clone MIB-1 (IR62; Dako UK Ltd.) for 1 h at room temperature. After two more washes in wash buffer FLEX, DAKO EnvIsion FLEX/HRP SM802 (K8000; Dako UK Ltd.) was added for 20 min at room temperature. Then, after a series of two washings with wash buffer FLEX, the staining was visualized by adding diaminobenzidine (DAB) (Dako UK Ltd.) for 10 min at room temperature. The slides were washed well in wash buffer FLEX and counterstained with EnVision FLEX HEMATOXILIN SM806 (K8008; Dako UK Ltd.) for 5 min, washed once with wash buffer FLEX, then a second time with water, and then dehydrated, cleared, and mounted in distyrene plasticizer xylene (DPX). Positive and negative controls were performed with each batch of slides. Photomicrographs were taken through a Nikon eclipse E400 microscope (Nikon France S.A, Champigny sur Marne, France) coupled to a QICAM Fast 1394 digital camera (QImaging, Roper Engineering s.r.o., Ostrava, Czech Republic).

Statistical Analysis. Statistical analysis was performed by Student's test (*t* test) (Microsoft Excel 2003). $p \leq 0.05$ was considered significant (*); $p \leq 0.01$ (**); $p \leq 0.001$ (***).

RESULTS AND DISCUSSION

Design and Synthesis of Arginine-Terminated TEA-Core PAMAM Dendrimers. The strategy used to synthesize arginine-decorated dendrimers is illustrated in Scheme 1. The synthesis began with the amine-terminated TEA-core PAMAM dendrimers and was followed by relevant transformations to covalently conjugate arginine building units to the dendrimer terminals. The amine-terminated PAMAM dendrimers from generations 1 to 4 ($\mathbf{G_1}$–$\mathbf{G_4}$) were prepared according to the procedure previously reported by our group.[12−14] These dendrimers were then coupled with the protected arginine precursor, Fmoc-Arg(pbf)-OH, in the presence of HOBt/HBTU. Subsequent removal of the Fmoc groups upon treatment with piperidine, followed by the deprotection of the pbf groups using TFA/TIS/water, delivered the desired arginine-decorated dendrimers from generation 1 to 4 ($\mathbf{G_1Arg}$–$\mathbf{G_4Arg}$) with excellent yields (Supporting Information).

The conjugation of arginine residues to the amine-terminated dendrimers was confirmed by the results of NMR analysis. For example, the ^{1}H NMR spectrum of the arginine-terminated generation 4 dendrimer ($\mathbf{G_4Arg}$) revealed the characteristic NMR signals corresponding to the arginine component at 1.7 ppm, 1.9 ppm, 3.3 ppm, and 4.0 ppm (Figure 2A). These signals were distinct from those of the corresponding amine-terminated generation 4 dendrimer ($\mathbf{G_4}$), and their presence thus acknowledged the successful appendage of arginine residues. Likewise, the characteristic ^{13}C NMR signals relating to the arginine residues were found at 24 ppm, 28 ppm, 40 ppm, 53 ppm, 157 ppm, and 171 ppm in the ^{13}C NMR spectrum of $\mathbf{G_4Arg}$ (Figure 2C), further affirming the attachment of arginine residues onto the dendrimer surface. We need to mention that additional control experiments carried out using the amine-terminated PAMAM dendrimer and Fmoc-Arg(pbf)-OH in the absence of the coupling reagents HOBt/HBTU could not deliver the corresponding arginine-conjugated dendrimer (data not shown).

Effective Delivery of siRNA with the Generation 4 Dendrimer $\mathbf{G_4Arg}$. After obtaining the arginine-terminated TEA-core dendrimers from generations 1 to 4, we then evaluated their ability to deliver an siRNA targeting heat shock protein 27 (Hsp27) into human castration-resistant prostate cancer PC-3 cells (Figure 3A). Hsp27 is a molecular chaperone playing an important role in drug resistance and has been recently considered as a novel target for treating drug-resistant prostate cancer, for which there is no efficacious treatment.[31,32] Gratifyingly, generation 4 of arginine-decorated dendrimer ($\mathbf{G_4Arg}$) exhibited remarkable down-regulation of Hsp27 protein (Figure 3A), which is comparable to that of the commercial transfection vector oligofectamine and our best performing TEA-core PAMAM dendrimer of generation 7 ($\mathbf{G_7}$). Such great improvement of gene silencing efficacy resulting from $\mathbf{G_4Arg}$-mediated siRNA delivery could only have been ascribed to the presence of the arginine terminals, as no significant gene silencing was observed with the same generation dendrimer $\mathbf{G_4}$ devoid of arginine terminals (Figure 3A).[15] Noteworthy is that the arginine-terminated dendrimers

dx.doi.org/10.1021/bc4005156 | *Bioconjugate Chem.* XXXX, XXX, XXX−XXX

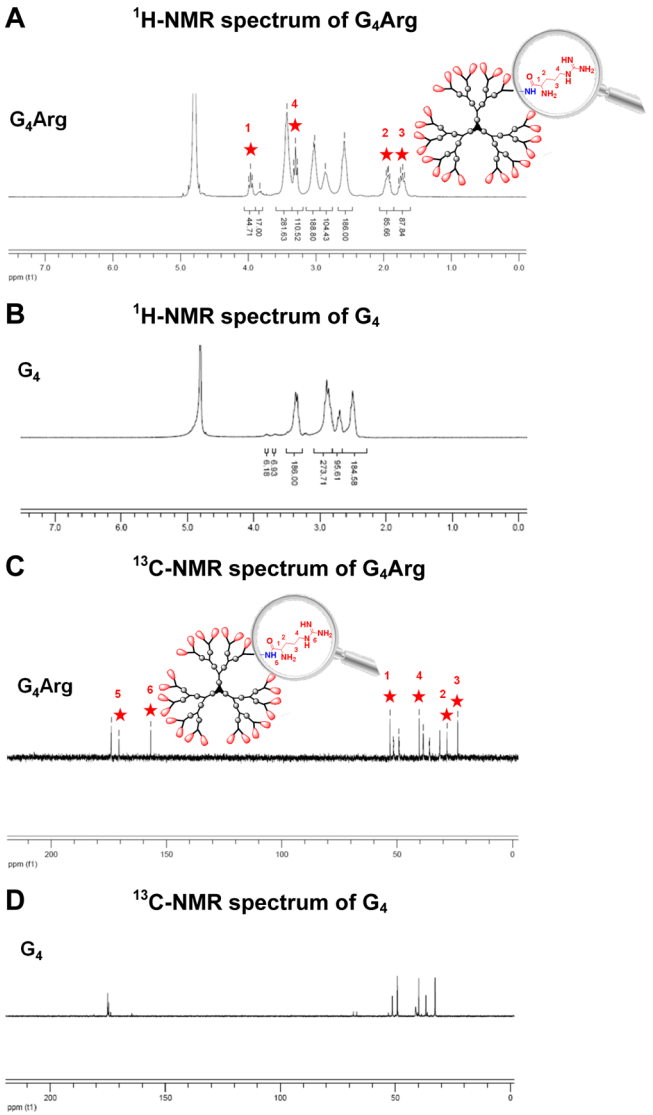

Figure 2. ^{1}H- and ^{13}C NMR spectra of **G$_4$Arg** and **G$_4$**. The peaks marked with a red star belong to the characteristic NMR signals of arginine residues.

of lower generation from **G$_1$Arg** to **G$_3$Arg** showed no siRNA-delivering activity. This can be ascribed to their structural features associated with a lower generation, which cannot provide the sufficient multivalency and cooperativity required to efficiently interact with the siRNA molecules and fulfill the task of transporting them along the journey to the desired site for gene silencing.

Importantly, the gene silencing resulting from **G$_4$Arg**-mediated siRNA delivery is specific, as no notable gene silencing at both mRNA (Figure 3B) and protein levels (Figure 3C) was observed with scramble siRNA delivered by **G$_4$Arg** under the same condition as **G$_4$Arg** with siRNA, neither with dendrimer alone nor siRNA alone. We also examined the serum effects on **G$_4$Arg**-mediated Hsp27 siRNA delivery. In the presence of FBS, the gene-silencing efficiency was decreased, possibly due to the interaction between serum proteins and siRNA/dendrimer complexes, thus destabilizing the siRNA/dendrimer complexes. Nevertheless, the serum effect could be minimized by increasing the N/P ratio to form more stable siRNA/dendrimer complexes, hence achieving significant gene silencing even in the presence of 10% FBS (Figure 3D).

Furthermore, the gene silencing with **G$_4$Arg** as the delivery vector was effective in different cell lines including prostate cancer PC-3 and C4-2 cells as well as breast cancer MDA-MB231 cells and showed dose-dependence with Hsp27 siRNA (Figure 3E), while no significant gene silencing was induced by **G$_4$Arg** with scramble siRNA, **G$_4$Arg** alone, and Hsp27 siRNA alone (Figure S1A, Supporting Information). In order to further confirm the efficiency of **G$_4$Arg**-mediated siRNA delivery, we assessed gene silencing using **G$_4$Arg** to deliver siRNA targeting translationally controlled tumor protein (TCTP), a protein which is implicated in many biological processes including cell growth, tumor reversion, induction of pluripotent stem cells, or apoptosis.[33,34] As demonstrated in Figure 3F, dose-dependent gene silencing of TCTP was observed, with more than 80% suppression of TCTP protein being attained with 50 nM siRNA at an N/P ratio of 10 in all three tested cell lines. Importantly, under the same condition as **G$_4$Arg** with siRNA, no notable gene silencing was induced with scramble siRNA delivered by **G$_4$Arg** as well as **G$_4$Arg** alone and siRNA targeting TCTP in the absence of **G$_4$Arg** in all three tested cell lines (Figure S1B, Supporting Information).

Collectively, these results demonstrate that the arginine-decorated generation 4 dendrimer (**G$_4$Arg**) is indeed effective and specific for siRNA delivery and hold great potential for further in vivo applications. Compared with the high generation dendrimer **G$_7$**, **G$_4$Arg** has a much more precisely controlled synthesis and greatly facilitated molecular characterization and quality control, constituting a promising candidate for further evaluation.

Enhanced Cellular Uptake Ability via Conjugation with Arginine Residues. To understand how the arginine-terminated dendrimer **G$_4$Arg** exhibits such superior high efficiency compared to its nonarginine dendrimer counterpart **G$_4$**, we first scrutinized the formation of siRNA/**G$_4$Arg** complexes (also called dendriplexes) before inspecting their cell uptake, which is the first essential step for successful siRNA delivery.

We used the electrophoresis mobility shift assay to examine the ability of **G$_4$Arg** to form a complex with siRNA. Stable complex formation was confirmed by **G$_4$Arg**, completely retarding siRNA migration at an N/P ratio of as low as 1.2 (Figure 4A), which is at least 4-fold and 2-fold more effective than the nonarginine bearing dendrimer **G$_4$** (N/P > 5) and our most potent dendrimer vector **G$_7$** (N/P > 2.5), respectively (Figure S2, Supporting Information).[35] The superior binding ability of **G$_4$Arg** toward siRNA can be explained by the simultaneous presence of two positive charges from the primary amine (pK_a = 9.0) and the guanidine group (pK_a = 12.5) per arginine residue, which permits a stronger interaction with siRNA. Further results obtained from dynamic light scattering (DLS) revealed that the siRNA/**G$_4$Arg** complexes existed as uniform nanoparticles with an average size of around 130 nm (Figure 4B). This is remarkably different from the corresponding counterpart **G$_4$**, which was unable to form stable and uniform nanoparticles with siRNA (data not shown). Additional zeta potential measurement affirmed that the siRNA/**G$_4$Arg** complexes exhibited positive zeta potential values around +26.2 mV (±0.7), suggesting the sustained colloidal stability of the siRNA/**G$_4$Arg** complexes. Altogether, these results demonstrate that the arginine-decorated dendrimer **G$_4$Arg** is effective at interacting with siRNA to form stable and uniform nanoparticles, in a much more efficient manner than the parent amine-terminated dendrimer **G$_4$**. The ready and

dx.doi.org/10.1021/bc4005156 | *Bioconjugate Chem.* XXXX, XXX, XXX−XXX

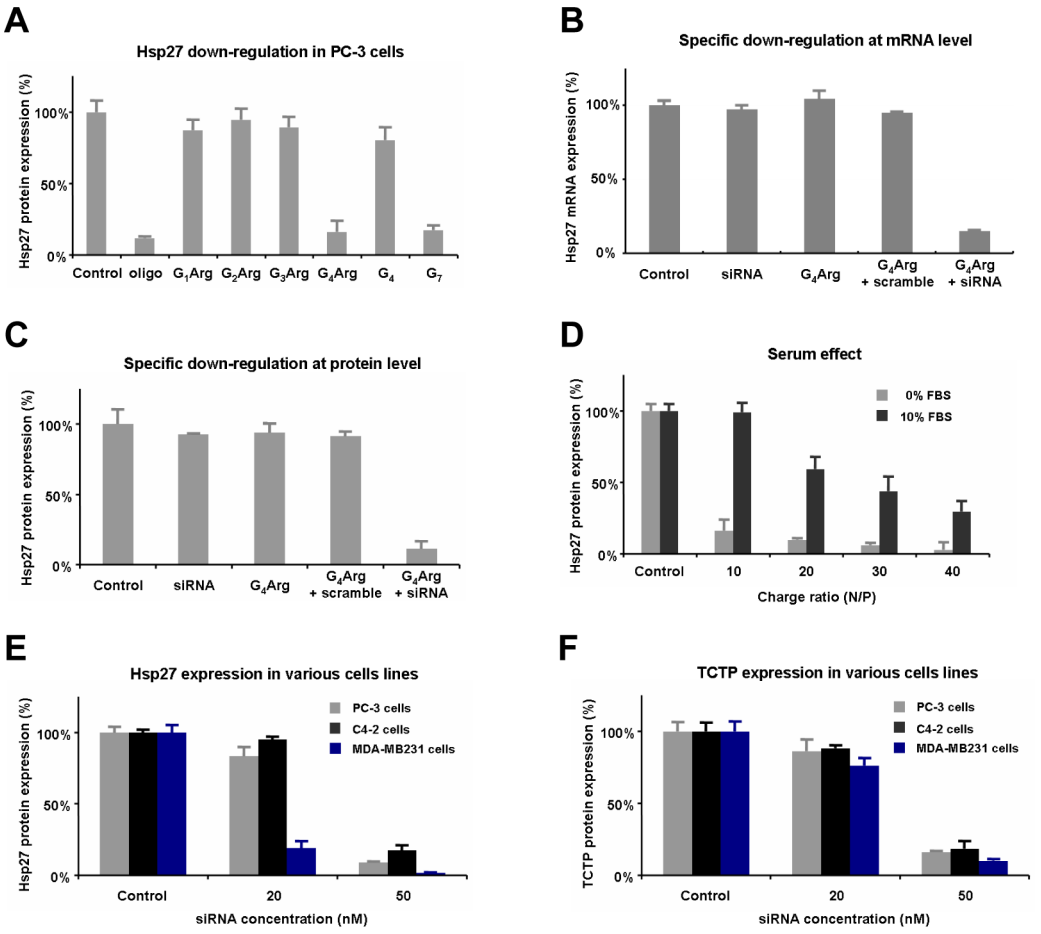

Figure 3. Dendrimer-mediated siRNA delivery and gene silencing of heat shock protein 27 (Hsp27) in human prostate cancer PC-3 cells at an N/P ratio of 10 with 50 nM Hsp27 siRNA, using commercial vector oligofectamine (oligo) as a positive control (A). **G_4Arg**-mediated delivery of Hsp27 siRNA produced gene silencing at the target mRNA (B) and a protein level (C) on PC-3 cells at an N/P ratio of 10 with 50 nM siRNA, using nontreatment, siRNA alone, **G_4Arg** alone, and scramble/**G_4Arg** as controls. (D) Serum effect on a **G_4Arg**-mediated delivery system using 50 nM Hsp27 siRNA with varying N/P ratios in the presence of 10% FBS. **G_4Arg**-mediated delivery of siRNA to target Hsp27 (E) and translationally controlled tumor protein (TCTP) (F) in different cancer cell lines with different concentrations of siRNA at an N/P ratio of 10. Quantification of Hsp27 or TCTP protein three days post-treatment, relative to no treatment as a control using Western blot.

uniform packing of siRNA into nanoparticles is of paramount importance for its cellular uptake and delivery.

We next studied the cellular uptake of the siRNA/dendrimer nanoparticles using flow cytometry with far-red fluorochrome Dy647-labeled siRNA. The fluorescent intensity of cells treated with siRNA/**G_4Arg** was significantly greater than that with siRNA/**G_4** (Figure 4C), giving prominence to the enhanced cellular uptake ability of siRNA/**G_4Arg** complexes compared with their counterpart siRNA/**G_4**. This could be ascribed to the positively charged guanidinium on arginine residues forming, via bidentate hydrogen bonding, particularly strong and important hydrogen bond networks with the negatively charged cell membrane constituents such as carboxylates, phosphates, and sulfates.[36] Such strong bond formation would promote their association with the cell membrane and allow such an escalated cross-membrane ability.[37,38] Consequentially, these results demonstrate that appending arginine residues on the dendrimer surface effectively improves the cellular uptake ability of the siRNA/**G_4Arg** dendriplex. This would explain why this strategy allowed even the low generation 4 arginine-terminated dendrimer (**G_4Arg**) to transport siRNA, whereas the amine-terminated dendrimer counterpart **G_4** was devoid of any notable delivery activity for siRNA.

Proton Sponge Effect Conserved in G_4Arg for Efficient siRNA Release. One other important consideration in the design of an efficient siRNA delivery vector is the adequate dissociation and release of the siRNA from the siRNA/vector complex once inside the cell. PAMAM dendrimer nanovectors are generally considered to effectively release their nucleic acid cargo via the proton sponge effect. This notion is based on the presence of a large number of tertiary amines within the PAMAM dendrimer which can be protonated in acidic endosomes, causing the endosomes to swell and finally burst to release the cargo.[39] We thus wished to test whether this proton sponge effect is also involved in the **G_4Arg**-mediated delivery system.

We first analyzed the pH titration profile of **G_4Arg** (Figure 5A), which is an important prerequisite for the proton sponge effect. At the physiological pH 7.4, 63% of the protonable groups (90 out of a total 142) are protonated, presumably corresponding to the protonated guanidine and primary amine groups within the arginine residues at the dendrimer surface. At the endosomal pH 5.0, 89% of the protonable groups (126 out of the 142) are protonated, which would indicate a significant amount of the tertiary amines within the dendrimer interior also being protonated once all the guanidine and amine groups

dx.doi.org/10.1021/bc4005156 | *Bioconjugate Chem.* XXXX, XXX, XXX−XXX

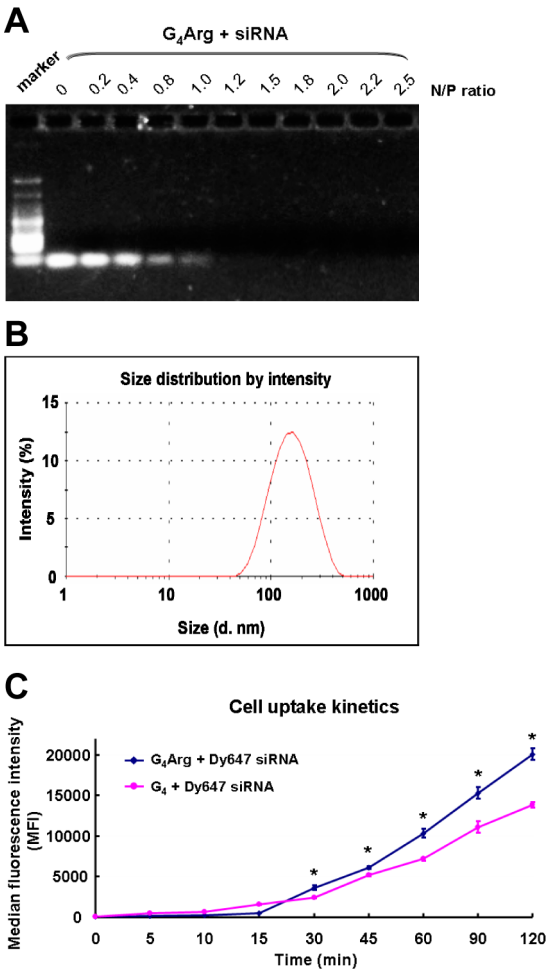

Figure 4. (A) Gel retardation of 200 ng of siRNA in agarose gel with **G_4Arg** at N/P charge ratios ranging from 0 to 2.5:1 in 50 mM Tris-HCl buffer pH 7.4. (B) Size and sized distribution of the siRNA/**G_4Arg** complexes at an N/P ratio of 10 determined using dynamic light scattering. (C) Cell uptake kinetics of the siRNA/dendrimer complexes in PC-3 cells evaluated using flow cytometric analyses at an N/P ratio of 10 with 50 nM siRNA. Experiments were carried out in triplicate. * differ from Dy647 siRNA/**G_4** complexes ($p \leq 0.05$) by Student's test.

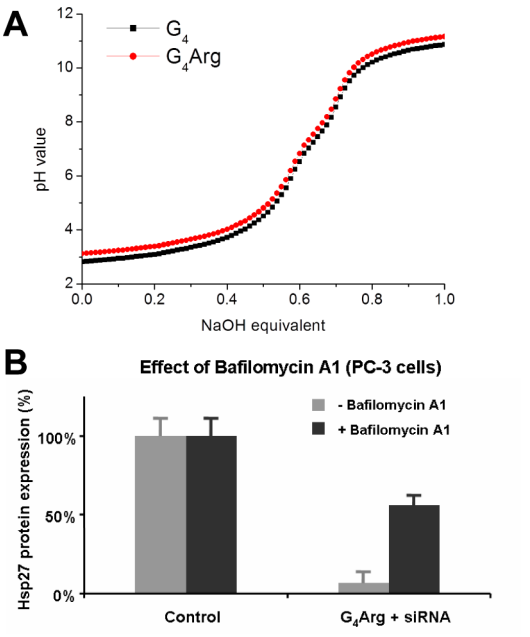

Figure 5. (A) Potentiometric pH back-titration profile of **G_4Arg** in comparison with that of **G_4**. (B) Bafilomycin A1, a proton pump inhibitor, decreases the **G_4Arg**-mediated gene silencing of Hsp27 using 50 nM siRNA and **G_4Arg** at an N/P ratio of 10 in PC-3 cells.

at the arginine terminals had been protonated. As shown in Figure 5A, **G_4Arg** displayed a continuous titration curve similar to that of **G_4**, implying that **G_4Arg** conserves the high buffering capacity of PAMAM dendrimers. All these findings represent advantageous properties for **G_4Arg** being able to eventually exercise a proton sponge effect for siRNA release.

We next evaluated the gene silencing effect in the presence of bafilomycin A1, a reagent frequently employed to study the proton sponge effect. Bafilomycin A1 is a proton pump inhibitor, which can selectively inhibit vacuolar H^+-ATPase and hence prevent acidification of endosomes. As shown in Figure 5B, the gene-silencing effect produced by **G_4Arg** with Hsp27 siRNA was considerably inhibited in the presence of bafilomycin A1. This strongly suggested the dependence of **G_4Arg**-mediated siRNA delivery on the endosomal acidification process and that the proton sponge effect contributed to the release of siRNA for effective gene silencing. This is in perfect agreement with the structural features of arginine-terminated PAMAM dendrimers, which contain a large number of tertiary amines within the interior, furnishing a robust buffering capacity and permitting a proton sponge effect for endosomal release.

Excellent Toxicity Profile of the G_4Arg-Mediated siRNA Delivery System. The potential toxicity of any new therapeutic candidate is a serious concern requiring rigorous assessment for the biomedical application.[40] With this in mind, we went on to evaluate the toxicity of **G_4Arg** for siRNA delivery using both a 3-(4,5-dimethylthiazol-2-yl)-2,5-diphenyl tetrazolium bromide (MTT) assay and a lactate dehydrogenase (LDH) assay. The MTT assay determines cell viability by measuring the cellular metabolic activity via NAD(P)H-dependent cellular oxidoreductase enzymes, whereas the LDH assay assesses cytotoxicity based on the loss of membrane integrity by determining the released LDH. Both methods are commonly used for assessing the cytotoxicity of nanoparticles. Compared with the no treatment control, no significant decrease in cell viability was observed following treatment with **G_4Arg** or with scramble siRNA/**G_4Arg** (Figure 6A) at an N/P ratio of 10, implying that there is no metabolic toxicity associated with the **G_4Arg** delivery system. In addition, neither **G_4Arg** nor scramble siRNA/**G_4Arg** induced LDH release at an N/P ratio of 10 (Figure 6B), suggesting no cell membrane damage. Further evaluation using both MTT and LDH assays (Figure 6C and D) of the toxicity of the **G_4Arg** delivery system with varying N/P ratios from 1/1 to 30/1 confirmed the excellent toxicity profile of **G_4Arg** over a broad range of N/P ratios. Altogether, these results clearly demonstrate that neither the dendrimer alone nor its complex with siRNA shows any notable metabolic toxicity or obvious damage to cell membrane integrity, thus establishing **G_4Arg** as a promising nanovector with high potential for further therapeutic application.

Functional siRNA Delivery Led to Effective Antiproliferative Activity in Prostate Cancer Models in Vitro and in Vivo. The excellent toxicity profile and the efficient siRNA delivery capacity of the **G_4Arg** dendrimer motivated us to further assess the therapeutic effect induced by **G_4Arg**-mediated

dx.doi.org/10.1021/bc4005156 | Bioconjugate Chem. XXXX, XXX, XXX−XXX

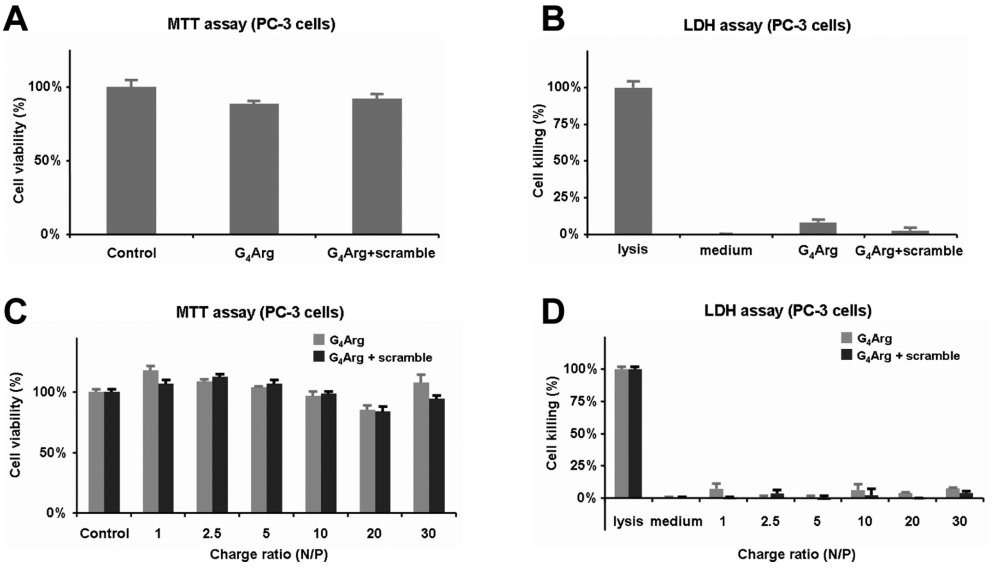

Figure 6. Toxicity profile of the **G_4Arg**-mediated delivery system was determined by the MTT (A,C) and LDH (B,D) assays with **G_4Arg** alone and scramble siRNA/**G_4Arg** in PC-3 cells either at an N/P ratio 10 or with varying N/P ratios.

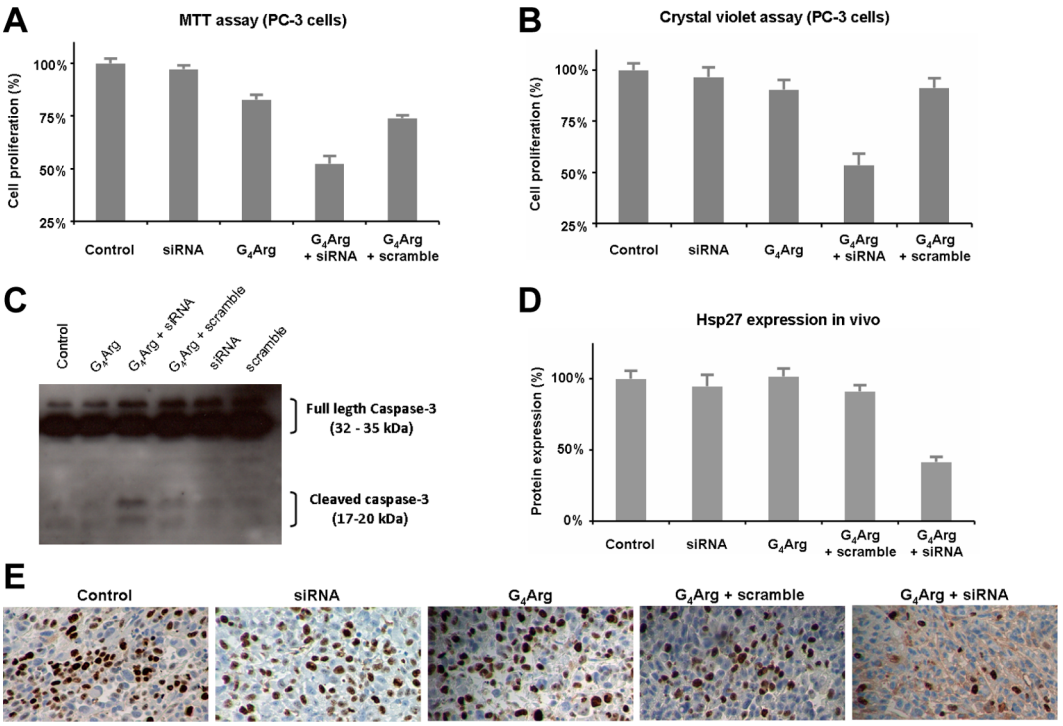

Figure 7. Functional siRNA delivery mediated by the **G_4Arg** dendrimer led to effective antiproliferative effects in prostate cancer models in vitro and in vivo. Cell proliferation of human prostate cancer PC-3 cells assessed by the MTT assay (A) and the crystal violet assay (B) six days post-treatment with 50 nM Hsp27 siRNA and **G_4Arg** at an N/P ratio of 10 on human prostate cancer PC-3 cells. (C) Caspase assay using Western blot analysis with caspase-3 antibody and cleaved caspase-3 antibody that recognizes full-length and cleaved caspase-3 three days post-treatment. PC-3 xenografted nude mice with intratumoral injection of siRNA/**G_4Arg** (3 mg·kg^{-1} siRNA and **G_4Arg** at an N/P ratio of 5) and PBS buffer, dendrimer alone, siRNA alone, and scramble siRNA/**G_4Arg** were used for in vivo evaluation during a period of two weeks with an injection frequency of twice a week (D and E). Effective gene silencing of Hsp27 (D) and the antiproliferation activity (E) in tumors after two weeks of treatment was assessed using Western blot and K_i-67 immunohistochemistry staining, respectively.

functional siRNA delivery using prostate cancer as a model. Prostate cancer is the most common cancer in men and the second leading cause of cancer death in industrialized countries.[41] While most patients initially respond to the first-line hormonal therapy, many become gradually resistant to hormonal and other conventional therapies, and no efficacious cure is yet available for advanced stages of the disease.[42,43] As we previously mentioned, Hsp27 is an interesting target for treating drug-resistant cancers including prostate cancer.[31,32] We therefore examined the anticancer activity resulting from treatment with the Hsp27 siRNA/**G_4Arg** dendriplex on prostate cancer PC-3 cells by assessing cell viability using the MTT (Figure 7A) and crystal violet (Figure 7B) assays. Compared to siRNA alone, **G_4Arg** alone, or scramble/**G_4Arg**,

dx.doi.org/10.1021/bc4005156 | Bioconjugate Chem. XXXX, XXX, XXX−XXX

which had no anticancer effect, treatment with Hsp27 siRNA/**G_4Arg** complexes led to specific and significant inhibition of cell proliferation (Figure 7A and B), alongside the observation of the induction of caspase cleavage (Figures 7C), indicating that the effective anticancer activity is the direct consequence of the siRNA-based gene silencing.

We next evaluated the **G_4Arg**-mediated siRNA delivery and the resulting gene silencing as well as antiproliferative activity in vivo using nude mice bearing PC-3 prostate cancer xenografts. Hsp27 siRNA/**G_4Arg** complexes were slowly injected into mice via intratumoral administration twice a week for 2 weeks. All mice survived well during and after the intervention and displayed no anxious or nervous behavior, and no acute toxicity was observed. Mice were sacrificed after two weeks of treatment, and the expression of Hsp27 in the tumors was measured using Western blotting analysis. Compared to the controls treated with PBS buffer, siRNA alone, **G_4Arg** alone, and the scrambled siRNA/**G_4Arg** complexes, the expression of Hsp27 protein was significantly down-regulated following treatment with Hsp27 siRNA/**G_4Arg** (Figure 7D), proving the direct consequence of an effective RNAi response in vivo following the delivery of Hsp27 siRNA mediated by **G_4Arg**. Immunohistochemical analysis using K_i-67 antibody staining revealed the significantly stronger inhibition of cancer cell proliferation in tumors derived from mice treated with Hsp27 siRNA/**G_4Arg** compared to those treated with scramble siRNA/**G_4Arg** and other controls (Figure 7E). Overall, these results demonstrate that **G_4Arg** is an effective vector to mediate siRNA delivery and produce a potent and specific RNAi response in vitro and in vivo, and thus illustrate its great promise in siRNA delivery for further clinical applications.

CONCLUSIONS

siRNA-based RNA interference (RNAi) is expected to offer an attractive means to sequence-specifically and efficiently silence disease-associated genes for treating various diseases. Notwithstanding, the implementation of RNAi-based therapeutics into a clinical setting is critically dependent on the development of safe and efficient delivery systems, which can improve the pharmacokinetic properties of siRNA and overcome the various barriers preventing their successful delivery. In this context, dendrimers have attracted considerable attention as nonviral nanovectors for siRNA delivery by virtue of their well-defined structures and multivalent features. In our quest to develop safe and efficient vectors for the delivery of siRNA therapeutics, we have previously demonstrated that high generations of structurally flexible PAMAM dendrimers bearing a triethanolamine (TEA) core are excellent nanovectors to deliver RNA therapeutics in different disease models. However, the large-scale synthesis of high generation dendrimers to GMP grade has proved technically challenging.

To circumvent this drawback, we developed in this work a strategy to confer lower generation TEA-core PAMAM dendrimers with the efficient siRNA delivery via conjugation of arginine units on the dendrimer terminals. We aimed to combine and harness the unique siRNA delivery properties of the structurally flexible dendrimers and the cell-penetrating advantages of arginine-rich motifs to enhance the cell membrane penetration and foster delivery efficiency. Interesting, the arginine-terminated TEA-core generation 4 PAMAM dendrimer (**G_4Arg**) proved to be effective at delivering siRNAs, leading to potent gene silencing both in vitro and in vivo. Further investigation confirmed that the dendrimer **G_4Arg** was bestowed with a superior capacity to form stable dendriplexes with siRNA and enhance cell uptake, resulting in significantly magnified gene silencing by comparison with its amine-terminated dendrimer counterpart **G_4**. Moreover, our delivery system **G_4Arg** displayed no discernible toxicity and was able to deliver siRNA in prostate cancer models both in vitro and in vivo, producing significant gene silencing and potent anticancer activity. All these findings demonstrate that (1) decoration of the dendrimer surface with arginine residues is an effective strategy to improve the delivery ability of dendrimers; and (2) our **G_4Arg** is a highly promising nanovector for efficacious siRNA delivery and holds great potential for further therapeutic applications. In addition, it is also to note that the synthesis, characterization, and quality control of the low generation dendrimer **G_4Arg** will be greatly facilitated and more easily achieved by comparison to the higher generation dendrimer **G_7**. This is undoubtedly a technical advantage for all further translational research aimed at developing siRNA-based therapeutic interventions using this dendrimer nanovector to treat various cancers and other major human diseases. We are actively pursuing these therapeutic goals.

ASSOCIATED CONTENT

Supporting Information

Additional characterization data. This material is available free of charge via the Internet at http://pubs.acs.org.

AUTHOR INFORMATION

Corresponding Authors

* (X.L.) E-mail: xiaoxuan.liu@univ-amu.fr.
* (L.P.) E-mail: ling.peng@univ-amu.fr.

Notes

The authors declare no competing financial interest.

ACKNOWLEDGMENTS

This work was supported by Ministry of Science and Technology of China (No.2012AA022501), the international ERA-Net EURONANOMED European Research project DENANORNA, PACA Canceropôle, INCa, Wuhan University, Aix-Marseille University, CNRS, INSERM, Association pour la Recherche sur les Tumeurs de la Prostate (XL), Association Française contre les Myopathies (XL), and China Scholarship Council (CL), under the auspice of European COST Action TD0802 "Dendrimers in Biomedical Applications". We are grateful to Mr. Patrick Gibier, Mr. Jean-Christophe Orsoni, and all the other members in the animal facility of Centre de Recherche en Cancérologie de Marseille for their great help during the performance of in vivo experiments. We also thank Ms. Jeanne Thomassin Piana, Ms. Mélanie Bentobji, and Ms. Francine Azario Cheillan for their help with the immunohistochemistry and relevant analyses.

ABBREVIATIONS

CPPs, cell-penetration peptides; DAB, diaminobenzidine; DIPEA, *N*,*N*-diisopropylethylamine; DLS, dynamic light scattering; DMEM, Dulbecco's modified Eagle's medium; DPX, distyrene plasticizer xylene; FBS, fetal bovine serum; G, generation; GMP, good manufacture practice; HOBt, 1-hydroxybenzotriazole; HBTU, *O*-(benzotriazol-1-yl)-*N*,*N*,*N*′,*N*′-tetramethyluronium hexafluorophosphate; Hsp27, heat shock protein 27; LDH, lactate dehydrogenase; MTT, 3-(4,5-dimethylthiazol-2-yl)-2,5-diphenyl tetrazolium bromide;

OD, optical density; PAMAM, poly(amidoamine); PTGS, post-transcriptional gene silencing; RNAi, RNA interference; siRNA, small interfering RNA; TAT, trans-activator of transcription; TCTP, translationally controlled tumor protein; TEA, triethanolamine

REFERENCES

(1) Hannon, G. J. (2002) RNA interference. *Nature 418*, 244−251.

(2) de Fougerolles, A., Vornlocher, H.-P., Maraganore, J., and Lieberman, J. (2007) Interfering with disease: a progress report on siRNA-based therapeutics. *Nat. Rev. Drug Discovery 6*, 443−453.

(3) Castanotto, D., and Rossi, J. J. (2009) The promises and pitfalls of RNA-interference-based therapeutics. *Nature 457*, 426−433.

(4) Davidson, B. L., and McCray, P. B. (2011) Current prospects for RNA interference-based therapies. *Nat. Rev. Genet. 12*, 329−340.

(5) Alabi, C., Vegas, A., and Anderson, D. (2012) Attacking the genome: emerging siRNA nanocarriers from concept to clinic. *Curr. Opin. Pharmacol. 12*, 427−433.

(6) Shen, H., Sun, T., and Ferrari, M. (2012) Nanovector delivery of siRNA for cancer therapy. *Cancer Gene Ther. 19*, 367−373.

(7) Tan, S. J., Kiatwuthinon, P., Roh, Y. H., Kahn, J. S., and Luo, D. (2011) Engineering nanocarriers for siRNA delivery. *Small 7*, 841−856.

(8) Astruc, D., Boisselier, E., and Ornelas, C. (2010) Dendrimers designed for functions: from physical, photophysical, and supramolecular properties to applications in sensing, catalysis, molecular electronics, photonics, and nanomedicine. *Chem. Rev. 110*, 1857−1959.

(9) Liu, X., Rocchi, P., and Peng, L. (2012) Dendrimers as non-viral vectors for siRNA delivery. *New J. Chem. 36*, 256−263.

(10) Ravina, M., Paolicelli, P., Seijo, B., and Sanchez, A. (2010) Knocking down gene expression with dendritic vectors. *Mini-Rev. Med. Chem. 10*, 73−86.

(11) Liu, X., Liu, C., Catapano, C. V., Peng, L., Zhou, J., and Rocchi, P. (2013) Structurally flexible triethanolamine-core poly(amidoamine) dendrimers as effective nanovectors to deliver RNAi-based therapeutics. *Biotechnol. Adv.*, DOI: 10.1016/j.biotechadv.2013.08.001.

(12) Wu, J., Zhou, J., Qu, F., Bao, P., Zhang, Y., and Peng, L. (2005) Polycationic dendrimers interact with RNA molecules: polyamine dendrimers inhibit the catalytic activity of Candida ribozymes. *Chem. Commun.*, 313−315.

(13) Liu, X., Wu, J., Yammine, M., Zhou, J., Posocco, P., Viel, S., Liu, C., Ziarelli, F., Fermeglia, M., Pricl, S., Victorero, G., Nguyen, C., Erbacher, P., Behr, J.-P., and Peng, L. (2011) Structurally flexible triethanolamine core PAMAM dendrimers are effective nanovectors for DNA transfection in vitro and in vivo to the mouse thymus. *Bioconjugate Chem. 22*, 2461−2473.

(14) Zhou, J., Wu, J., Hafdi, N., Behr, J.-P., Erbacher, P., and Peng, L. (2006) PAMAM dendrimers for efficient siRNA delivery and potent gene silencing. *Chem. Commun.*, 2362−2364.

(15) Liu, X. X., Rocchi, P., Qu, F. Q., Zheng, S. Q., Liang, Z. C., Gleave, M., Iovanna, J., and Peng, L. (2009) PAMAM dendrimers mediate siRNA delivery to target Hsp27 and produce potent antiproliferative effects on prostate cancer cells. *ChemMedChem 4*, 1302−1310.

(16) Zhou, J., Neff, C. P., Liu, X., Zhang, J., Li, H., Smith, D. D., Swiderski, P., Aboellail, T., Huang, Y., Du, Q., Liang, Z., Peng, L., Akkina, R., and Rossi, J. J. (2011) Systemic administration of combinatorial dsiRNAs via nanoparticles efficiently suppresses HIV-1 infection in humanized mice. *Mol. Ther. 19*, 2228−2238.

(17) Lang, M. F., Yang, S., Zhao, C., Sun, G., Murai, K., Wu, X., Wang, J., Gao, H., Brown, C. E., Liu, X., Zhou, J., Peng, L., Rossi, J. J., and Shi, Y. (2012) Genome-wide profiling identified a set of miRNAs that are differentially expressed in glioblastoma stem cells and normal neural stem cells. *PLoS One 7*, e36248.

(18) Liu, X., Liu, C., Laurini, E., Posocco, P., Pricl, S., Qu, F., Rocchi, P., and Peng, L. (2012) Efficient delivery of sticky siRNA and potent gene silencing in a prostate cancer model using a generation 5 triethanolamine-core PAMAM dendrimer. *Mol. Pharmaceutics 9*, 470−481.

(19) Posocco, P., Liu, X., Laurini, E., Marson, D., Chen, C., Liu, C., Fermeglia, M., Rocchi, P., Pricl, S., and Peng, L. (2013) Impact of siRNA overhangs for dendrimer-mediated siRNA delivery and gene silencing. *Mol. Pharmaceutics 10*, 3262−3273.

(20) Reebye, V., Sætrom, P., Mintz, P. J., Huang, K. W., Swiderski, P., Peng, L., Liu, C., Liu, X. X., Jensen, S., Zacharoulis, D., Kostomitsopoulos, N., Kasahara, N., Nicholls, J. P., Jiao, L. R., Pai, M., Mizandari, M., Chikovani, T., Emara, M. M., Haoudi, A., Tomalia, D. A., Rossi, J. J., Habib, N. A., and Spalding, D. R. (2014) A novel RNA oligonucleotide improves liver function and inhibits liver carcinogenesis in vivo. *Hepatology 59*, 216−227.

(21) Brooks, H., Lebleu, B., and Vivès, E. (2005) Tat peptide-mediated cellular delivery: back to basics. *Adv. Drug Delivery Rev. 57*, 559−577.

(22) Dupont, E., Prochiantz, A., and Joliot, A. (2011) Penetratin story: an overview. *Methods Mol. Biol. 683*, 21−29.

(23) Wender, P. A., Mitchell, D. J., Pattabiraman, K., Pelkey, E. T., Steinman, L., and Rothbard, J. B. (2000) The design, synthesis, and evaluation of molecules that enable or enhance cellular uptake: peptoid molecular transporters. *Proc. Natl. Acad. Sci. U.S.A. 97*, 13003−13008.

(24) Futaki, S. (2005) Membrane-permeable arginine-rich peptides and the translocation mechanisms. *Adv. Drug Delivery Rev. 57*, 547−558.

(25) Choi, J. S., Nam, K., Park, J.-y., Kim, J.-B., Lee, J.-K., and Park, J.-s. (2004) Enhanced transfection efficiency of PAMAM dendrimer by surface modification with L-arginine. *J. Controlled Release 99*, 445−456.

(26) Kim, J.-B., Choi, J. S., Nam, K., Lee, M., Park, J.-S., and Lee, J.-K. (2006) Enhanced transfection of primary cortical cultures using arginine-grafted PAMAM dendrimer, PAMAM-Arg. *J. Controlled Release 114*, 110−117.

(27) Kwon, M. J., An, S., Choi, S., Nam, K., Jung, H. S., Yoon, C. S., Ko, J. H., Jun, H. J., Kim, T. K., Jung, S. J., Park, J. H., Lee, Y., and Park, J.-S. (2012) Effective healing of diabetic skin wounds by using nonviral gene therapy based on minicircle vascular endothelial growth factor DNA and a cationic dendrimer. *J. Gene Med. 14*, 272−278.

(28) Hirose, H., Takeuchi, T., Osakada, H., Pujals, S., Katayama, S., Nakase, I., Kobayashi, S., Haraguchi, T., and Futaki, S. (2012) Transient focal membrane deformation induced by arginine-rich peptides leads to their direct penetration into cells. *Mol. Ther. 20*, 984−993.

(29) Wright, L. R., Rothbard, J. B., and Wender, P. A. (2003) Guanidinium rich peptide transporters and drug delivery. *Curr. Protein Pept. Sci. 4*, 105−124.

(30) Nakase, I., Akita, H., Kogure, K., Gräslund, A., Langel, Ü., Harashima, H., and Futaki, S. (2012) Efficient intracellular delivery of nucleic acid pharmaceuticals using cell-penetrating peptides. *Acc. Chem. Res. 45*, 1132−1139.

(31) Rocchi, P., Beraldi, E., Ettinger, S., Fazli, L., Vessella, R. L., Nelson, C., and Gleave, M. (2005) Increased Hsp27 after androgen ablation facilitates androgen-independent progression in prostate cancer via signal transducers and activators of transcription 3-mediated suppression of apoptosis. *Cancer Res. 65*, 11083−11093.

(32) Rocchi, P., So, A., Kojima, S., Signaevsky, M., Beraldi, E., Fazli, L., Hurtado-coll, A., Yamanaka, K., and Gleave, M. (2004) Heat shock protein 27 increases after androgen ablation and plays a cytoprotective role in hormone-refractory prostate cancer. *Cancer Res. 64*, 6595−6602.

(33) Bommer, U.-A., and Thiele, B.-J. (2004) The translationally controlled tumour protein (TCTP). *Int. J. Biochem. Cell Biol. 36*, 379−385.

(34) Baylot, V., Katsogiannou, M., Andrieu, C., Taieb, D., Acunzo, J., Giusiano, S., Fazli, L., Gleave, M., Garrido, C., and Rocchi, P. (2012) Targeting TCTP as a new therapeutic strategy in castration-resistant prostate cancer. *Mol. Ther. 20*, 2244−2256.

(35) Shen, X. C., Zhou, J., Liu, X., Wu, J., Qu, F., Zhang, Z. L., Pang, D. W., Quéléver, G., Zhang, C. C., and Peng, L. (2007) Importance of

size-to-charge ratio in construction of stable and uniform nanoscale RNA/dendrimer complexes. *Org. Biomol. Chem. 5*, 3674−3681.
(36) Wender, P. A., Galliher, W. C., Goun, E. A., Jones, L. R., and Pillow, T. H. (2008) The design of guanidinium-rich transporters and their internalization mechanisms. *Adv. Drug Delivery Rev. 60*, 452−472.
(37) Rothbard, J. B., Jessop, T. C., Lewis, R. S., Murray, B. A., and Wender, P. A. (2004) Role of membrane potential and hydrogen bonding in the mechanism of translocation of guanidinium-rich peptides into cells. *J. Am. Chem. Soc. 126*, 9506−9507.
(38) Lättig-Tünnemann, G., Prinz, M., Hoffmann, D., Behlke, J., Palm-Apergi, C., Morano, I., Herce, H. D., and Cardoso, M. C. (2011) Backbone rigidity and static presentation of guanidinium groups increases cellular uptake of arginine-rich cell-penetrating peptides. *Nat. Commun. 2*, 453.
(39) Sonawane, N. D., Szoka, F. C., and Verkman, A. S. (2003) Chloride accumulation and swelling in endosomes enhances DNA transfer by polyamine-DNA polyplexes. *J. Biol. Chem. 278*, 44826−44831.
(40) Duncan, R., and Izzo, L. (2005) Dendrimer biocompatibility and toxicity. *Adv. Drug Delivery Rev. 57*, 2215−2237.
(41) Dhanasekaran, S. M., Barrette, T. R., Ghosh, D., Shah, R., Varambally, S., Kurachi, K., Pienta, K. J., Rubin, M. A., and Chinnaiyan, A. M. (2001) Delineation of prognostic biomarkers in prostate cancer. *Nature 412*, 822−826.
(42) Fusi, A., Procopio, G., Della Torre, S., Ricotta, R., Bianchini, G., Salvioni, R., Ferrari, L., Martinetti, A., Savelli, G., and Villa, S. (2004) Treatment options in hormone-refractory metastatic prostate carcinoma. *Tumori 90*, 535−46.
(43) Tannock, I. F., de Wit, R., Berry, W. R., Horti, J., Pluzanska, A., Chi, K. N., Oudard, S., Théodore, C., James, N. D., and Turesson, I. (2004) Docetaxel plus prednisone or mitoxantrone plus prednisone for advanced prostate cancer. *N. Engl. J. Med. 351*, 1502−1512.